

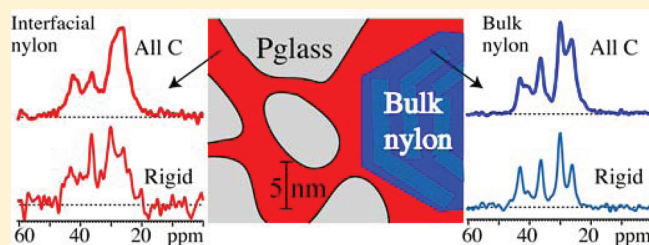
Reduced Crystallinity and Mobility of Nylon-6 Confined near the Organic–Inorganic Interface in a Phosphate Glass-Rich Nanocomposite Detected by ^1H – ^{13}C NMR

Aditya Rawal,[†] Xueqian Kong,[†] Yan Meng,[‡] Joshua U. Otaigbe,[‡] and Klaus Schmidt-Rohr^{*,†}

[†]Department of Chemistry, Iowa State University, Ames, Iowa 50011, United States

[‡]School of Polymers and High Performance Materials, University of Southern Mississippi, Hattiesburg, Mississippi 39406, United States

ABSTRACT: The effects of confinement of solid polyamide 6 in a nanocomposite with a rigid inorganic glass, a hybrid organic–inorganic material with potential applications in optoelectronics, gas/liquid barrier membranes, and heterogeneous catalysis, have been investigated by ^{13}C , ^1H – ^{13}C , and ^1H – ^1H solid-state nuclear magnetic resonance (NMR) spectroscopy. The material is synthesized by melt blending 90 vol % of a low- T_g tin fluorophosphate glass (Pglass) with 10 vol % polyamide 6 (PA6). ^{13}C NMR with selective spectroscopy of rigid and mobile segments shows a 2-fold suppression of the average crystallinity of PA6 in the composite. The reduction in crystallinity, to ca. 5%, is even more pronounced for PA6 near the interface with Pglass, as seen in selective ^{13}C spectra of PA6 near the organic–inorganic interface obtained by two-dimensional ^1H – ^{13}C correlation NMR. The spectrum after a ^{13}C T_1 filter indicates a reduced mobility of the interfacial PA6 polymer, which is in ~ 5 nm thick domains according to ^1H spin-diffusion experiments. The spectra prove that about half of the PA6 is in the nanocomposite, while the rest is bulklike in large domains. The presence of large domains is also deduced from incomplete ^1H spin exchange between PA6 and Pglass in the ^1H spin-diffusion experiments.



INTRODUCTION

Hybrids of tin fluorophosphate glass (“Pglass”) and various polymers, such as polyamide 6 (“nylon” or “PA6”), can display a rich tunable morphology during processing.¹ Nanoscale dispersions of the Pglass in the polymer phase² and a cocontinuous (interpenetrating) structure with unique periodicity and phase connectivity of the hybrid components have been observed.¹ These structures are dependent on factors such as type of polymer, concentration of Pglass, and processing (or mixing) conditions used.^{1,3} It was also discovered that the Pglass is miscible in the liquid state with certain polar organic polymers, including polyamides.³ This is thought to be facilitated by a strong interaction or reaction between the polar –NH– (amide) functional groups of the organic polymers and the –OH groups of the Pglass.³ Clearly, a fundamental understanding of the dispersion characteristics at molecular-level length scales and the dynamics of the hybrid Pglass/PA6 materials is crucial for their maximum exploitation in a number of application areas such as optoelectronics, gas/liquid barrier membranes, heterogeneous catalysis, and host materials for organic chromophores.

In one of our previous NMR studies of Pglass–PA6 hybrids, we provided proof of partial nanocomposite formation and characterized the inorganic component near the organic–inorganic interface.² The molecular and mechanical properties of the inorganic glass–polymer hybrid are governed by the interactions at the interfacial layers between the two components. In this

paper, we investigate the state of the polymer near the organic–inorganic interface in Pglass–PA6 hybrids using one- and two-dimensional solid-state ^{13}C and ^1H NMR to provide fundamental insights into the molecular structure and dynamics of the materials.

Effects of rigid interfaces on polymer dynamics have been the focus of many studies by NMR and other methods. For instance, evidence for a bound rubber layer on carbon black particles⁴ or an interfacial layer between soft and hard blocks of copolymers^{5,6} has been provided. However, these have mostly involved amorphous polymers above their bulk glass transition temperature and focused on the reduction in chain mobility. In this study, we analyze the effect of rigid interfaces on a semicrystalline polymer, focusing on the reduction in crystallinity. While some previous studies have deduced the mobility of segments in the interfacial layer in the presence of signals from bulklike material, the Pglass–nylon system and our two-dimensional NMR methodology enable us to selectively observe only the interesting interfacial components and characterize their properties.

In our previous work, we studied hybrid materials with a dominant polymer fraction;^{2,7} here, we focus on a material with 10 vol % polymer, where the interfacial components make up a larger fraction of the total polymer and can therefore be studied more

Received: July 29, 2011

Revised: September 8, 2011

Published: September 28, 2011

easily in terms of crystallinity, crystal modification, and segmental mobility, which can be assessed by ^{13}C NMR spectroscopy with relaxation-time filtering. At high Pglass concentration (≥ 70 vol %), a significant fraction of the polymer is in close contact with the rigid inorganic glass, while the small signal of this interfacial polymer would be overwhelmed in composites with a large fraction of bulk polymer. The spectrum of polymer near the organic–inorganic interface can be observed selectively in two-dimensional ^1H – ^{13}C NMR spectra. The length scale of polymer confinement, on the order of 10 nm, is estimated from analysis of ^1H spin-diffusion data.

EXPERIMENTAL SECTION

Materials. The low- T_g Pglass has a molar composition of 50% SnF_2 + 20% SnO + 30% P_2O_5 , a density of 3.75 g/cm^3 , and a T_g of $\sim 120 \pm 5\text{ }^\circ\text{C}$.^{8–10} The low- T_g Pglass was synthesized according to procedures reported by Tick⁸ and others.¹ The tin fluoride and tin oxide were supplied by Cerac, and the ammonium phosphate was purchased from Sigma-Aldrich. The polymer used was Capron 8270 HS, a polyamide 6 (nylon or PA6), supplied by Allied Signal. The hybrids were prepared using a Thermo-Haake Polydrive Melt Mixer equipped with roller rotor blades. Prior to melt-mixing, the Polydrive mixer was heated to $250\text{ }^\circ\text{C}$ and allowed to equilibrate for at least 20 min. The PA6 was added to the Polydrive first and allowed to mix for 5 min to obtain a homogeneous melt. The Pglass was then added, and the two components were allowed to mix together for 10 min. Hybrid samples containing, by volume, 90% Pglass and 10% PA6 (90:10 composite) and 70% Pglass and 30% PA6 (70:30 composite) were made for analysis. In order to avoid effects of grinding on the structure, the samples were investigated by NMR as large chunks of millimeter dimensions, packed into 7 mm NMR rotors with approximate $C_{nv>2}$ symmetry for balance.

NMR Parameters. Solid-state 1D single-pulse ^1H NMR, cross-polarization (CP) MAS ^{13}C NMR without and with a 5 s ^{13}C T_1 filter,⁷ direct-polarization ^{13}C NMR with 2 s recycle delay, and ^1H – ^{13}C heteronuclear correlation (HetCor) NMR experiments were conducted on a Bruker DSX-400 NMR spectrometer, with a 9.4 T wide-bore superconducting magnet, operating at frequencies of 400 MHz for ^1H and 100 MHz for ^{13}C . The measurements were performed under conditions of 6 kHz MAS using Bruker 4 mm H-X-Y triple-resonance and 7 mm H-X double-resonance MAS probe heads in zirconia rotors with Kel-F caps. The 90° pulse lengths for the ^{13}C and ^1H nuclei were 4 μs .

^1H wide-line spectra were acquired after a single short pulse using a simple probe-head background suppression scheme,¹¹ while for higher resolution, frequency-switched Lee–Goldburg (FSLG) homonuclear decoupling¹² was applied. Two-dimensional ^1H – ^1H correlation experiments with spin diffusion were performed to obtain information on proximity between ^1H associated with Pglass and PA6 in the hybrids. ^1H magnetization is allowed to evolve for an incremented time t_1 with homonuclear FSLG decoupling prior to storage along the z -axis for a time t_{sd} before being returned back to the x – y plane for detection (without decoupling). During t_{sd} , ^1H spin diffusion occurs and distributes the magnetization to more distant protons; the time scale of the diffusion process gives an estimate of the nanoscale size of the components.

Two-dimensional ^1H – ^{13}C HetCor experiments provide selective ^{13}C spectra of the PA6 segments close to the Pglass. FSLG homonuclear decoupling was applied during the ^1H evolution period. Regular Hartmann–Hahn cross-polarization, with a contact time of 1 ms, was used to transfer the ^1H magnetization from ^1H in Pglass, identified by their 7 ppm chemical shift, to nearby ^{13}C for detection. In order to enhance the ^1H signal associated with the Pglass, ^1H spin diffusion from Pglass to nylon was introduced before cross-polarization. The small volume fraction ($\sim 5\%$) of nylon near the interface with Pglass makes

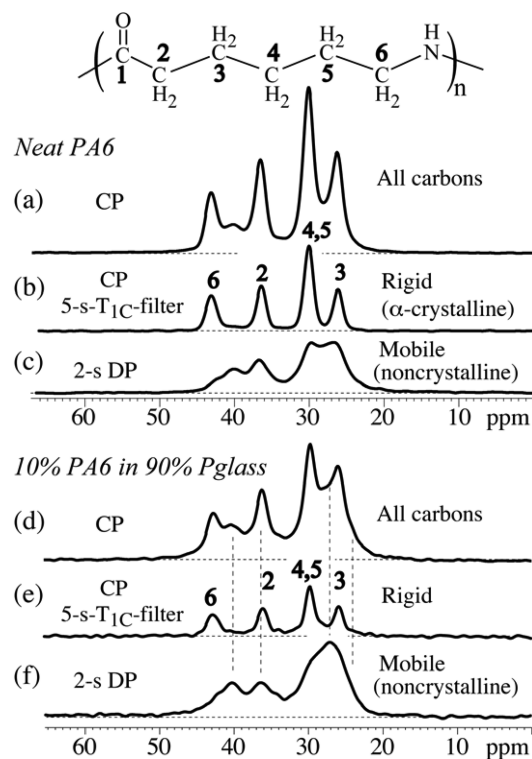


Figure 1. ^{13}C NMR spectra (alkyl region) of PA6 (a–c) in neat PA6 and (d–f) in the 90:10 Pglass:PA6 composite, after (a, d) cross-polarization (CP) from ^1H ; (b, e) CP and a 5 s T_{1C} filter, which selects signals of crystalline regions; and (c, f) direct polarization with a 2 s recycle delay, which selects signals of mobile noncrystalline regions.

these experiments challenging in terms of sensitivity. Each 2D HetCor spectrum required 1 day of measuring time.

RESULTS AND DISCUSSION

Reduced PA6 Crystallinity in the Composite. Figure 1 compares ^{13}C CP-MAS spectra of the alkyl carbons in neat PA6 (from ref 7) and in the 90:10 composite material. The spectra in Figure 1a,d are nonselective and show carbon species in both ordered (crystalline) and disordered (amorphous) environments, as indicated by a combination of narrow and broad peaks. This is expected, since PA6 is a semicrystalline polymer of 40% crystallinity.⁷ Comparison of Figures 1a and 1d shows that PA6 in the composite exhibits the narrow peaks in a significantly smaller proportion than neat PA6, indicating a strongly reduced polymer crystallinity in the composite.

The crystalline fraction has a structure that maximizes the extent of intermolecular $\text{N–H}\cdots\text{O}=\text{C}$ hydrogen bonding and chain packing. Therefore, the polymer segments in the crystallites have less molecular mobility than those in the amorphous regions. The T_1 (spin–lattice) relaxation of ^{13}C nuclei is a sensitive probe of molecular dynamics in the MHz regime, and the ^{13}C spin–lattice relaxation time T_{1C} of the crystallites can be much greater than that of the amorphous regions. This difference in the T_{1C} relaxation times can be used in a T_{1C} filter¹³ to select the signals of the crystalline PA6.⁷ As shown in Figures 1b,e, a 5 s T_{1C} filter effectively suppresses the signal of the amorphous component, retaining mostly the sharp resolved peaks characteristic of the crystalline α -modification.^{7,14} In the composite, a low,

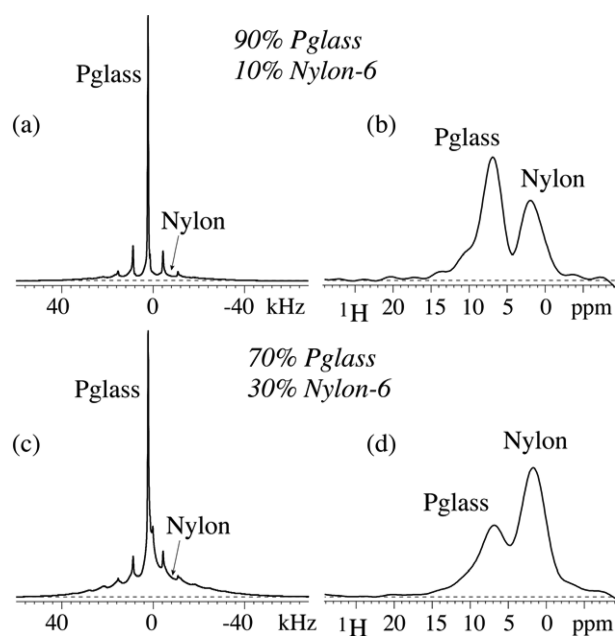


Figure 2. ^1H NMR spectra of composites of Pglass and nylon in (a, b) 90:10 and (c, d) 70:30 volume ratio. (a, c) Wide-line spectra with probehead background suppression;¹¹ (b, d) spectra with FSLG homonuclear decoupling.

broad signal component is also retained, seen most prominently at around 26 ppm. This will be shown below to be a feature of the PA6 near the interface with Pglass. The spectral contribution of the crystalline signals in the composite is only about half as large as in neat PA6, which indicates a reduction in crystallinity by about a factor of 2, to around 20%. No significant peaks of crystallites of the γ -modification, which are clustered between 30 and 40 ppm and were observed previously in PA6–Pglass composites with a high polymer concentration,⁷ are detected in the spectra.

The fast $T_{1\rho}$ relaxation of the amorphous components means that their signals can be observed selectively in a ^{13}C MAS experiment with direct polarization using a short recycle delay, e.g., of 2 s. This is shown in Figures 1c and 1f, where only broad peaks of amorphous components in PA6 are observed.

The spectra of Figure 1 demonstrate that the presence of Pglass reduced the polymer crystallinity. In the following, we will show that the reduction in crystallinity for PA6 near the organic–inorganic interface is even more drastic and that the spectra in Figures 1d–f are superpositions of (at least) two semicrystalline PA6 components in the composite.

^1H NMR of the Hybrid Material. In order to selectively characterize the structure and dynamics of PA6 segments near the interface with Pglass, it is necessary for the PA6 and Pglass ^1H species to be spectroscopically distinct, for example in terms of their chemical shift, line width, or T_1 relaxation time. In Figure 2, we show that the ^1H spectra of the Pglass–PA6 composites indeed show the required distinct features of the two components.

^1H NMR spectra of polymers in the solid state are generally broad due to the effects of ^1H – ^1H dipolar couplings,¹⁵ which are an order of magnitude greater than the dispersion of ^1H chemical shifts. This broadening can provide contrast from the protons dispersed in Pglass, which have only weak ^1H – ^1H couplings and

therefore present sharp lines. Figure 2 shows the regular ^1H solid-state NMR spectra of the 90:10 and 70:30 Pglass:PA6 hybrids (Figures 2a and 2c). They are composed of at least two spectral components. A narrow peak centered at 7 ppm is superimposed on a strongly dipolar broadened band. The broad signal corresponds to alkyl species associated with high ^1H density, i.e., the PA6. The narrow 7 ppm peak is associated with the component of low ^1H density, i.e., the Pglass; this is tentatively assigned to H_2O in Pglass.² The intensity of the broad nylon peak in Figure 2c is significantly reduced compared to that in Figure 2a, which reflects the 3-fold reduced nylon concentration in the material. The difference in the line widths is related to the significantly different concentrations of the ^1H species in the organic and inorganic regions and thus their dipolar broadening. Nevertheless, for a certain fraction of noncrystalline organic component, motional averaging of ^1H dipolar couplings can result in reduced line width similar to that of Pglass protons. Therefore, differences in the line widths of the ^1H species may not be a reliable method of discrimination between the organic and inorganic components.

Instead, we can exploit differences in ^1H chemical shifts, which are unaffected by mobility. In order to resolve the ^1H chemical shifts of organic and inorganic components, the ^1H NMR spectra were also acquired with frequency-switched Lee–Goldburg (FSLG) irradiation, which removes the ^1H – ^1H dipolar couplings and enhances spectral resolution (see Figures 2b,d). The alkyl ^1H peak of PA6 at 2 ppm is quite well resolved from the Pglass peak at 7 ppm.² The relative intensities of the Pglass and PA6 peaks, which are much more similar than their volume fractions, show that the density of ^1H species in the PA6 is higher than in the Pglass, as expected.

^{13}C Spectra of Interfacial PA6. Selective ^{13}C NMR spectra from only the interfacial PA6 component within the 90:10 hybrid can be obtained from two-dimensional ^1H – ^{13}C heteronuclear correlation (HetCor) NMR spectra. In these spectra, the ^{13}C and ^1H frequencies are spread into a 2D map, which correlates specific ^{13}C species and ^1H species. Most importantly, ^{13}C signals associated with ^1H of Pglass must be from nylon segments near the organic–inorganic interface. Figure 3a shows three 2D ^1H – ^{13}C HetCor spectra of the 90:10 composite, with 0.5, 5, and 50 ms of ^1H spin diffusion before cross-polarization. The ^1H projections from the ω_1 dimension are plotted in Figure 3b for the different spin-diffusion times. The ^1H spectra show an increase in the intensity of the Pglass peak at 7 ppm, which corresponds to ^1H spin diffusion from Pglass to PA6. While the peak at 7 ppm has a significant contribution from the amide proton of PA6 at the shortest spin diffusion time, after 50 ms it is predominantly from the Pglass. Figure 3c shows ^{13}C slices from the 2D spectra at the ^1H chemical shift of 2 ppm, characteristic of PA6.

Selective spectra of ^{13}C near Pglass are shown in Figure 3d, obtained as cross sections from the 2D spectra in Figure 3a at the Pglass ^1H chemical shift of 7 ppm. The ^1H magnetization originates in Pglass and is detected in nylon, which is only possible for nylon near the organic–inorganic interface. The sharp signals of crystalline PA6 are much reduced or even not recognizable in these ^{13}C spectra. This is evidence of greatly reduced crystallinity, to near 5%, in the interfacial component compared to neat PA6 (Figure 1a) and the composite on average (Figures 1d and 3c). The spectral pattern, with strong intensity near 26 and 42 ppm, does not match that of the crystalline γ -modification, whose signals are all concentrated between 30 and 40 ppm.⁷

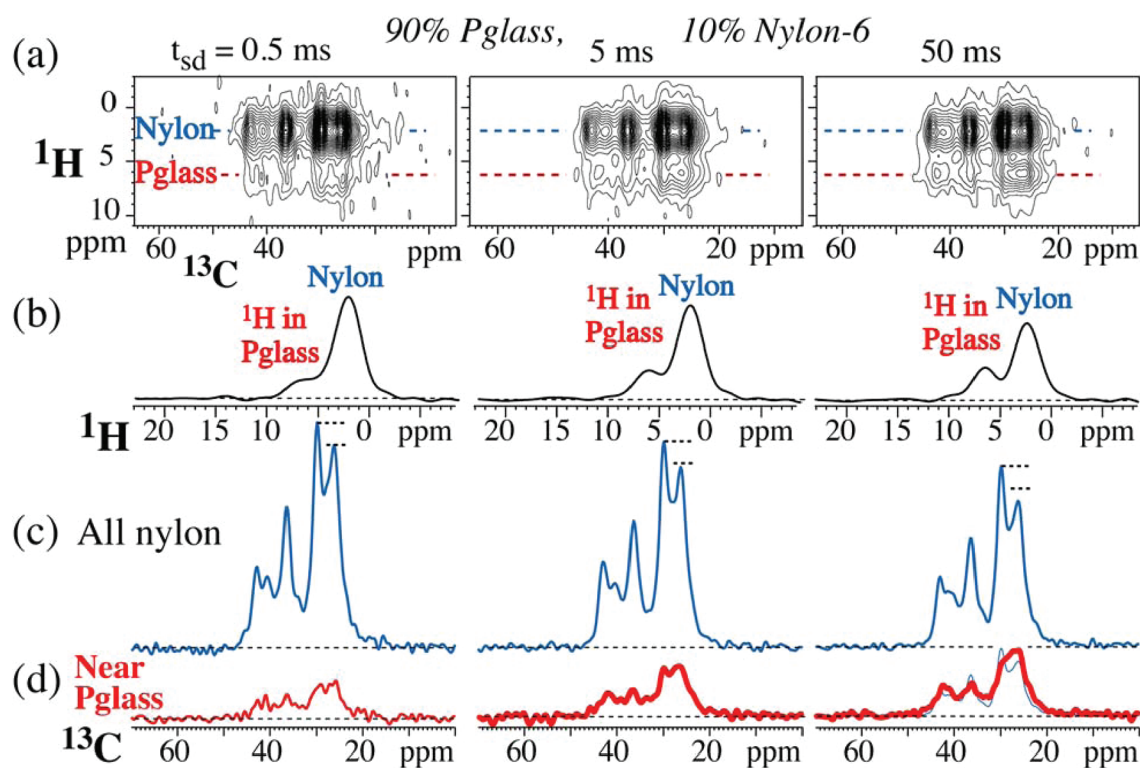


Figure 3. (a) Two-dimensional ^1H – ^{13}C NMR spectra (alkyl region) of composites of Pglass and nylon in a 90:10 volume ratio, for spin-diffusion times t_{sd} of 0.5, 5, and 50 ms. (b) Corresponding projections of the 2D spectra onto the ^1H dimension. (c) Cross sections along the ^{13}C dimension at 2 ppm ^1H chemical shift (nylon). Short horizontal dashed lines highlight the decreased relative height of the peak at 26 ppm. (d) Cross section along the ^{13}C dimension at 7 ppm ^1H chemical shift (Pglass). In the 50 ms spectrum, the spectrum from (c) is shown superimposed (thin line).

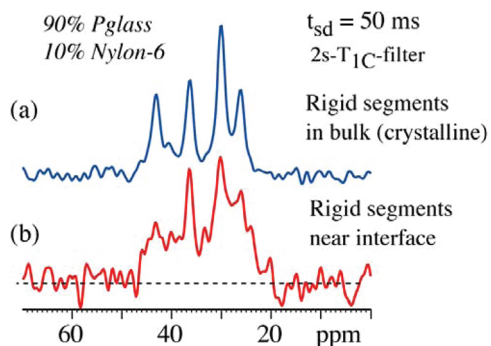


Figure 4. Cross sections along the ^{13}C dimension at (a) the nylon (2 ppm) and (b) the Pglass (7 ppm) ^1H chemical shift position from a two-dimensional ^1H – ^{13}C NMR spectra after spin-diffusion time of 50 ms and a 2 s T_1 filter to select signals of rigid segments. The spectra have been scaled to the same maximum peak height.

Concomitant with the increase of the intensity at the right end of the ^{13}C spectra, near 26 ppm, in Figure 3d, the corresponding intensity decrease can be recognized in the 2 ppm cross sections (Figure 3c). It is manifested as a decreasing height of the signal at 26 ppm, relative to the largest peak, with mixing time, highlighted by short horizontal dashed lines in Figure 3c. An amount of nylon ^1H magnetization equal to the small exchange peak in Figure 3b has diffused into Pglass. As a result, this contribution of interfacial nylon, most prominently near 26 ppm, is removed from the signal at 2 ppm in Figure 3c.

Rigid Segments at the Interface. The spectrum of the interfacial nylon in Figure 3d shows strong signatures of the amorphous component. Nevertheless, peaks reminiscent of the crystalline α -phase are detected near the left end of the spectrum, where neither the amorphous component nor the crystalline γ -modification shows any signal.⁷

In order to assess whether crystallites are present near the interface, we added a 2 s T_1 filter to the ^1H – ^{13}C HetCor experiment with $t_{\text{sd}} = 50$ ms. The filter suppresses the signals of mobile noncrystalline regions. Figures 4a and 4b show the cross sections at 2 and 7 ppm ^1H chemical shift, respectively. Again, the ^{13}C slice from 2 ppm represents predominantly the rigid bulk PA6, showing mostly the narrow peaks of the rigid crystalline α -phase, while the ^{13}C slice at 7 ppm represents exclusively the rigid interfacial PA6. Even for the interfacial components, the maximum is now at the position of the most prominent peak of the crystalline α -phase. This shows that some crystallites are present.

Nevertheless, most of the spectral area in Figure 4b is found in broad spectral bands. This indicates reduced molecular mobility of the disordered interfacial PA6 component, which can be attributed to the influence of the rigid Pglass nearby. Thus, the structural constraints imposed on the PA6 by rigid Pglass not only prevent it from forming ordered crystallites but also limit the molecular motion of the induced amorphous structure.

Thickness of Confined PA6 Domains in the Pglass–PA6 Composite. The ^{13}C and ^1H – ^{13}C NMR spectra have shown pronounced effects of the Pglass on the nylon crystallinity and mobility. The thickness of the PA6 domains in the nanocomposite can be estimated by ^1H spin diffusion NMR, which is also an

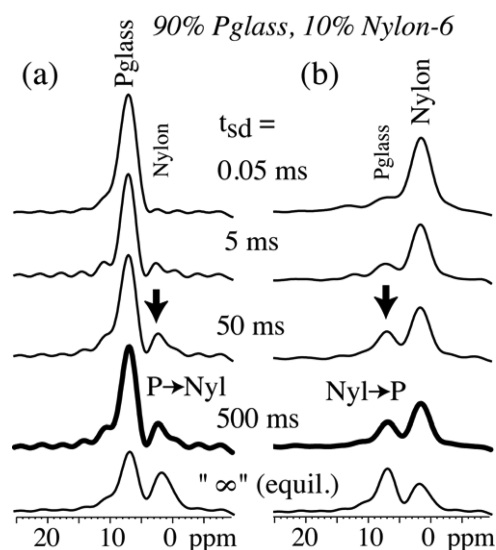


Figure 5. Cross sections from two-dimensional ^1H NMR spectra with homonuclear dipolar decoupling during t_1 , of composites of Pglass and nylon in 90:10 volume ratio, as a function of spin-diffusion time t_{sd} . (a) Cross sections at the sharp peak of Pglass in the ω_2 dimension. (b) Cross sections from nylon signal between the sharp sidebands of the Pglass signal. At the bottom, the regular 1D spectrum, scaled to equal area as the spectra above it, is shown as a placeholder for the spectrum after full equilibration.

excellent method for proving that a nanocomposite has been formed.^{2,16,17} Unlike electron microscopy, this NMR method is not dependent on contrast in electron density. It only requires appreciable concentrations of spectrally distinct ^1H species, which is the case for the Pglass–PA6 composites studied here (see Figure 2). The ^1H spin diffusion between the PA6 and the Pglass has been measured with high resolution in a 2D ^1H – ^1H correlation experiment for the 90:10 Pglass–PA6 composite. 1D slices along the ω_1 dimension extracted from the 2D experiment show the ^1H spin diffusion between the two components (see Figure 5).

The 1D slices at the sharp 7 ppm peak in the ω_2 dimension, corresponding to the Pglass ^1H species (Figure 5a), monitor the spin diffusion from the PA6 to the Pglass ^1H species. On the other hand, the 1D cross sections taken in the broad band of nylon in the ω_2 dimension (Figure 5b) show the spin diffusion from the Pglass to the PA6 ^1H species. It is interesting to note that ^{13}C detection in the ^1H – ^{13}C HetCor spectra of Figure 2, which only sees polymer signal since the inorganic glass contains no carbon, corresponds to the selection of nylon signal in Figure 5b. The spin diffusion time is varied from 0.05 to 500 ms. The unselective 1D ^1H FSLG spectra from Figure 4, which can be considered to represent completely equilibrated ^1H magnetization between the Pglass and the PA6, are shown at the bottom of the spin-diffusion series, scaled to equal area as the spectra above them.

The spectra show exchange peaks (marked by bold arrows in Figure 5), indicating significant diffusion of magnetization from Pglass to PA6 and vice versa, within 5 ms of spin diffusion, confirming nanocomposite formation. With increasing spin-diffusion time, the exchange peak intensity grows asymptotically toward its maximum. Increasing the spin-diffusion time from 50 to 500 ms does not significantly change the exchange peak intensities. This shows that there is a component with PA6 and Pglass nanodomains,

whose thickness corresponds to the distance covered by ^1H spin diffusion in less than 50 ms. The thickness d_A of the polymer domains can be estimated based on the time of saturation $t_{\text{sd}}^s \approx 20$ ms, the proton fraction $f_B \approx 0.6$ of the Pglass in the nanocomposite, and the effective spin diffusion coefficient $D_{\text{eff}} \approx 0.2 \text{ nm}^2/\text{ms}$,¹⁸ according to^{18,19}

$$d_A = \frac{\varepsilon}{f_B} \sqrt{\frac{4}{\pi} D_{\text{eff}} t_{\text{sd}}^s} \quad (1)$$

Depending on whether we assume polymer layers ($\varepsilon = 1$) or cylindrical structures ($\varepsilon = 2$), eq 1 yields a thickness of 3.5 or 7.5 nm of the PA6 domains. Given the uncertainties in the parameters, we should say that the thickness of the PA6 domains is around 5 nm.

Estimate of the Nanocomposite Fraction. The fact that spin diffusion cannot equilibrate the magnetization even within 500 ms indicates the presence of domains of >50 nm thickness. Whether these are large domains of polymer or of Pglass, or of both, is not obvious from the ^1H spectra.²⁰ However, the difference in the ^{13}C spectra associated with the two ^1H peaks in Figure 3 documents the presence of a significant fraction of bulklike PA6 in large domains: If the interfacial component were the only type of nylon present, the ^{13}C spectral patterns in Figure 3 at both ^1H peak positions would be the same. From the spectra, and the 2-fold reduction in PA6 crystallinity in the composite, relative to neat PA6, we estimate that about half of PA6 is in a nanocomposite and half in large domains. Further, microscopy has shown that the 90:10 composite, with its large fraction of Pglass, contains large Pglass domains.

From the intensity of the long-time exchange peaks, limits on the fraction of material in the nanocomposite can be estimated.²⁰ For a pure nanocomposite with proton fractions f_A and f_B of components A and B (Pglass and PA6, respectively), both of the equilibrated (long-time) exchange peaks have the same intensity of $f_{\text{ex}} = f_A \times f_B$ (if the selected signals are taken to have initial intensities of f_A and f_B , as shown in Figure 5). If only fractions $f_{c,A}$ and $f_{c,B}$ of the components A and B are in the nanocomposite, with the remainder of the material in large domains that produce negligible cross-peak intensity, the long-time exchange peak intensity is²⁰

$$f_{\text{ex}} = f_{c,A} f_A \times f_{c,B} f_B / (f_{c,A} f_A + f_{c,B} f_B) \quad (2)$$

Material in large domains not participating in spin diffusion then results in a reduction of the exchange peak intensity by a factor

$$R = f_{\text{ex}} / f_A \times f_B = f_{c,A} \times f_{c,B} / (f_{c,A} f_A + f_{c,B} f_B) \quad (3)$$

which can be read off from the peak intensities in the two bottom rows in Figure 5; the bottom spectrum has been scaled to give an exchange peak intensity of $f_A \times f_B$, so the relative intensity of the actual long-time exchange peak is R . Comparison of the spectra in the two bottom rows of Figure 5 shows $R \approx 0.5$.

The proton fractions, $f_A = 0.6$ for Pglass and $f_B = 1 - f_A = 0.4$ for PA6, are known, so eq 3 contains two unknowns, $f_{c,A}$ and $f_{c,B}$. The ^{13}C NMR data presented above indicate that close to half of polymer is in large domains, $f_{c,B} \approx 0.5$. Then, eq 3 gives an estimate of the Pglass fraction in the nanocomposite:

$$f_{c,A} = f_{c,B} f_B R / (f_{c,B} - R f_A) \approx 0.5 \quad (4)$$

In summary, this analysis of the spin-diffusion data indicates that the nanocomposite accounts for roughly half of the hybrid material, and large domains of both PA6 and Pglass make up

the other half. This is similar to the results of our studies of polymer-rich Pglass–PA6 composites.²

Possible Origins of Reduced Crystallinity. Our study has shown that about half of the PA6 in the composite with Pglass has a very low crystallinity and a reduced mobility. These Pglass domains are thin, with a thickness of only ~5 nm. The suppression of crystallinity can be attributed at least in part to the small thickness of the polymer layer, which is comparable to the width of a crystalline lamella and less than the polymer radius of gyration. These constraints on the polymer can interfere with the formation of crystalline lamellae. The Pglass–PA6 interactions also have the potential to reduce the molecular dynamics during crystallization and disrupt the polymer–polymer H-bonding (C=O–H–N) necessary for crystallite formation. In addition, Pglass, whose glass-transition temperature is lower than the melting and heterogeneous-nucleation temperature of PA6, cannot provide a solid surface to nucleate polymer crystal growth. The molecular dynamics of short-range and long-range Pglass structures in this temperature range²¹ may disrupt PA6 crystal formation in the hybrid material.

CONCLUSIONS

One- and two-dimensional ¹³C and ¹H NMR techniques have been used to investigate the structure and dynamics of 10 vol % polyamide 6 (PA6) in a composite with 90% inorganic tin fluorophosphate glass (Pglass). ¹³C NMR with selection of the crystalline and amorphous fractions based on *T*₁ρ differences shows that the PA6 crystallinity in the composite is reduced 2-fold (to ~20%). Bulklike PA6 in large domains accounts for about half of the polymer and PA6 in the nanocomposite for the other half. The PA6 near the interface with Pglass, observed selectively in two-dimensional ¹H–¹³C spectra, has very low crystallinity (~5%). ¹H spin-diffusion NMR measurements reveal that the PA6 in the nanocomposite is constrained to ~5 nm thick domains within a Pglass matrix. Increased rigidity of the interfacial amorphous PA6 is observed and attributed to the constraining effect of the Pglass surface. These confinement-induced effects of the Pglass on the PA6 structure may affect the materials properties relevant in a number of applications including optoelectronics, gas/liquid barrier membranes, and heterogeneous catalysis.¹

AUTHOR INFORMATION

Corresponding Author

*E-mail: srohr@iastate.edu.

ACKNOWLEDGMENT

We acknowledge the U.S. National Science Foundation for financial support of this research under Awards DMR-0652400 and DMR-0652350. J.U.O. gratefully acknowledges the research work of his former graduate students and postdocs.

REFERENCES

- (1) Urman, K.; Otaigbe, J. U. *Prog. Polym. Sci.* **2007**, *32*, 1462–1498.
- (2) Rawal, A.; Urman, K.; Otaigbe, J. U.; Schmidt-Rohr, K. *Chem. Mater.* **2006**, *18*, 6333–6338.
- (3) Urman, K.; Otaigbe, J. *J. Polym. Sci., Part B: Polym. Phys.* **2005**, *44*, 441–450.
- (4) Berriot, J.; Lequeux, F.; Monnerie, L.; Montes, H.; Long, D.; Sotta, P. *J. Non-Cryst. Solids* **2002**, *307*, 719–724.

- (5) Thomann, Y.; Thomann, R.; Hasenhiindl, A.; Mulhaupt, R.; Heck, B.; Knoll, K.; Steininger, H.; Saalwachter, K. *Macromolecules* **2009**, *42*, 5685–5699.
- (6) Gandhi, S.; Melian, C.; Demco, D. E.; Brar, A. S.; Blumich, B. *Macromol. Chem. Phys.* **2008**, *209*, 1576–1585.
- (7) Rawal, A.; Fang, X. W.; Urman, K.; Iverson, D.; Otaigbe, J. U.; Schmidt-Rohr, K. *J. Polym. Sci., Part B: Polym. Phys.* **2008**, *46*, 857–860.
- (8) Tick, P. *Phys. Chem. Glasses* **1984**, *25*, 149–154.
- (9) Xu, X. J.; Day, D. E. *Phys. Chem. Glasses* **1990**, *31*, 183–187.
- (10) Xu, X. J.; Day, D. E.; Brow, R. K.; Callahan, P. M. *Phys. Chem. Glasses* **1995**, *36*, 264–271.
- (11) Chen, Q.; Hou, S. S.; Schmidt-Rohr, K. *Solid State Nucl. Magn. Reson.* **2004**, *26*, 11–15.
- (12) Bielecki, A.; Kolbert, A. C.; Levitt, M. H. *Chem. Phys. Lett.* **1989**, *155*, 341–346.
- (13) Torchia, D. A. *J. Magn. Reson.* **1978**, *30*, 613–616.
- (14) Hatfield, G. R.; Glans, J. H.; Hammond, W. B. *Macromolecules* **1990**, *23*, 1654–1658.
- (15) Schmidt-Rohr, K.; Clauss, J.; Spiess, H. W. *Macromolecules* **1992**, *25*, 3273–3277.
- (16) Hou, S. S.; Bonagamba, T. J.; Beyer, F. L.; Madison, P. H.; Schmidt-Rohr, K. *Macromolecules* **2003**, *36*, 2769–2776.
- (17) VanderHart, D. L.; Asano, A. *Macromolecules* **2001**, *34*, 3819–3822.
- (18) Clauss, J.; Schmidt-Rohr, K.; Spiess, H. W. *Acta Polym.* **1993**, *44*, 1–17.
- (19) Schmidt-Rohr, K.; Spiess, H. W. *Multidimensional Solid-State NMR and Polymers*; Academic Press: London, 1994.
- (20) Caravatti, P.; Neuenschwander, P.; Ernst, R. R. *Macromolecules* **1985**, *18*, 119–122.
- (21) Tischendorf, B. C.; Alam, T. M.; Cygan, R. T.; Otaigbe, J. U. *J. Non-Cryst. Solids* **2003**, *316*, 261.